International Journal of Engineering Research & Technology (IJERT)
ISSN: 2278-0181
Vol. 3 Issue 8, August - 2014

Modelling Stress Concentration Effects in Unidirectional Glass Fibre-Reinforced Polymer Composites

Abdalla M. Abdalla[1], Ahmed Abdel-Moneim[1] & Mohamed N. A. Nasr[1,2,*]
[1]Dept. of Materials Science & Engineering, Egypt-Japan University of Science & Technology, EGYPT
[2]Dept. of Mechanical Engineering, Faculty of Engineering, Alexandria University, EGYPT

***Abstract* — In the present study, finite element modelling has been used to examine the stress concentration effects of having a central hole in unidirectional glass fibre-reinforced polyester (GFRP) laminates, under tensile loading. Special focus has been given to the load carrying capacity, in terms of defining an equivalent stress concentration factor (K_T), and sample initial stiffness. A virgin model (without a central hole) has been used as a basis for evaluating the stress concentration effects. In addition, progressive failure features, before complete failure, have been modelled with the aid of the multi-continuum theory (MCT). Two ply-orientations were examined; $[0/90]_{2s}$ and $[\pm45]_{2s}$ laminates. The model was first validated using previously published experimental data. The results were explained in terms of local stress state, compared to simple mechanics of materials basics, and agreed with previously published results.**

Keywords* — *Stress concentration; unidirectional; glass fibre-reinforced polyester (GFRP); finite element modelling (FEM); open-hole; ply-orientation.

I. INTRODUCTION

A. Background and Literature Review

Fibre-reinforced polymer (FRP) composites are currently being widely used. Their use has been on the rise especially in the automotive and aerospace sectors. It is a well-known fact that the main advantage of composite materials, in general, is their high stiffness-to-weight and strength-to-weight ratios. A special advantage of FRP composites is the possibility to tailor their mechanical properties by controlling their fibre orientation and fibre volume fraction (V_f), as fibres are their main load carrying element. For the same reason, unidirectional composites have predominant mechanical properties in only one direction (the fibre direction).

In the absence of accurate prediction methods (analytical and / or numerical), the optimization process of composites structures using experimental techniques would be extremely difficult and expensive. This is mainly due to the large number of parameters that control their performance and need to be addressed [1]. Even though predicting the ultimate strength of composite materials is of a crucial importance, it remains to be a challenge because there is no method, so far, that can perfectly predict failure characteristics of FRP composites, especially in complex cases [2,3].

Multiple failure criteria have been developed that were basically developed based on extensive experimental testing of unidirectional FRP composite laminates. This includes, for example; Hankinson, Strussi, Norris–Fischer, Kopnov, Tsai-Hill, Norris-Interaction, Hill, Norris-Distortional, Tsai-Hahn and Cowin criteria [4,5]. These criteria are commonly used mainly because of their simplicity and relatively good accuracy [6]. It is important to note that, the aforementioned analytical criteria only predict damage initiation, and are not capable of predicting progressive failure of FRP laminates.

Chang and Chang [7] were the first to propose a two-dimensional model based on progressive damage analysis (PDA), using finite element modelling (FEM) to simulate the failure processes of FRP laminates and predict their ultimate strengths. Tan [8] and Tan and Perez [9] further developed Chang's method and examined a wide range of degradation. Camanho [10], Shokrieh [11,12] and Tserpes [13] established three-dimensional finite element (FE) models to perform PDA on FRP laminates, where the material stiffness was degraded according to the damage modes encountered. Most of the aforementioned PDA used constant values for material degradation factors, which can also be called damage factors. These parameters were determined experimentally or defined empirically. Lapczyk and Hurtado [14] established a two-dimensional progressive damage model (PDM) adopting the continuum damage mechanics (CDM), with linear material degradation factors.

As part of the mechanical characterization of composite laminate joints, the open-hole tensile test is used to determine their mechanical strength. The open-hole tensile strength is an important parameter that limits the load carrying capability and controls the damage mechanics of those laminates, especially for riveted and bolted joints [15]. The damage and fracture mechanisms of composite laminates containing holes are highly complicated due to the stress concentration effects, as well as the interaction between various stress components. Since glass fibre-reinforced polymer composite laminates are widely used in several applications, several analytical, numerical and experimental works were carried out in order to determine their open-hole tensile strength.

As part of the experimental investigation of the mechanical strength of open-hole samples, Yashiro et al. [16] introduced embedded Fibre Bragg Grating (FBG) sensors into a cross-ply laminate with an open hole to predict their damage patterns. Suemasu et al. [17,18] studied the damage initiation and growth in quasi-isotropic composite laminates

with a central hole in compression. In addition, Sadeghi et al. [19] performed progressive matrix cracking damage analysis for symmetric laminates, with a number of plies incorporating central hole under in-plane tensile/shear loading conditions. O'Higgins et al. [20] compared the open-hole tensile strength of carbon fibre-reinforced polymer (CFRP) to that of high-strength S2-glass fibre-reinforced polymer (GFRP) laminates. Dan-Jumbo et al. [21] have carried out a study on strength prediction of graphite/epoxy laminates with multiple holes. In addition, other progressive damage models have been developed for different unidirectional FRP laminates with central holes under tensile loading [22, 23, 24, 25].

Due to the complex mechanical behaviour of open-hope FRP laminates, their damage mechanics, and the difficulty of relying solely on experimental techniques to understand such behaviour; the present work focuses on modelling progressive failure of open-hole unidirectional FRP laminates under tensile loading. This is done using FEM, with the aid of the multi-continuum theory (MCT), explained below. The commercial FE software Abaqus/Standard 6.12 was used. The stress concentration effects of having a central hole in unidirectional GFRP laminates at two fibre orientations are examined. Two types of samples were used; $[0/90]_{2s}$ and $[\pm 45]_{2s}$ laminates. The current model has been validated, and the results were compared to previously published data and simple mechanics of materials basics.

B. *Multi-continuum Theory (MCT)*

Failure of composite materials normally starts at the constituent level and may, indeed, be limited to simply one constituent or extend over different constituents. Typical conventional modelling techniques treat composite lamina as a homogeneous solid with uniform properties [26]. However, the MCT approach is a multi-scale continuum mechanics approach that starts with the classical micromechanics-based strain decomposition technique of Hill [27], and incorporates it in a numerical algorithm that allows volume average constituent (fibre and matrix) stresses to be extracted from homogenized composite stresses. The constituents are treated as independent yet connected continua, where their responses can be determined and assessed [28]. When the MCT approach is used in FEM, material failure is modelled via stiffness degradation, where a fraction of the original un-failed constituent stiffness is assigned to it when failure occurs. In other words, when failure occurs, the elastic properties of the failed constituent are degraded and, correspondingly, the composite elastic properties are appropriately degraded [29]. Mayes et al. [30] examined using the MCT approach in FEM of progressive failure of different unidirectional continuous fibre composite laminates, under uniaxial and multiaxial loading conditions. Comparing the predicted stress-strain curves to their corresponding experimental curves showed very good match.

Moreover, the MCT methodology offers an ultimate combination of accuracy and efficiency for determining damage initiation and predicting damage propagation. In response to the lack of practical tools for progressive failure simulation, Firehole Composites has developed the Intelligent Discrete Softening Method (IDSM) [31]. Developed specifically for analysis of composite materials, this simulation technology offers two major advantages over previously available solutions: First, it drastically increases convergence strength which allows the whole load history of a structure to be effectively simulated. Second, it improves the reliance on small load increments which allows the entire simulation to be finished utilizing far less load increments.

II. FINITE ELEMENT MODELLING (FEM)

A. *Model Description*

In order to predict the stress concentration effects in unidirectional GFRP composites, two FE models were built. The first model (Model *A*) represents the standard open-hole tensile test sample, as per ASTM D5766, where the sample has a central hole that induces stress concentration effects. Figure 1 shows the geometry and boundary conditions of Model *A*; sample thickness (not shown) is 2.5 mm. The sample is loaded at one end in a displacement-controlled manner, and fixed at the other. ASTM D5766 identifies the width-to-hole diameter ratio and hole diameter-to-thickness ratio to be 6 and 2.4, respectively. The second model (Model *B*) represents a plain "virgin" sample without any stress concentration effects; i.e., no central hole. Model *B* has the same exact dimensions as Model *A*, except for the hole. It is important to note that, ASTM D5766 only specifies sample dimensions with no preference to number of plies. Accordingly, based on experimental trials and previously published data, an 8-ply sample was modelled. In order to evaluate the stress concentration effects at different fibre orientations, two types of laminates were modelled; $[0/90]_{2S}$ and $[\pm 45]_{2S}$. This was done for both models; Model *A* and Model *B*. The commercial FE platform ABAQUS/Standard V6.12, along with Autodesk Simulation Composite Analysis (ASCA) plugin, was used in the current work.

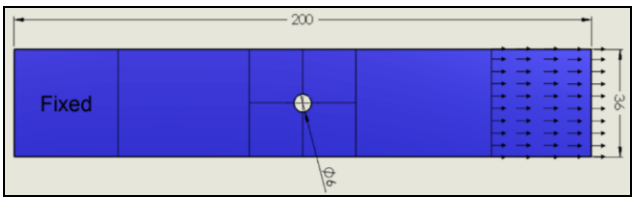

Figure 1: Model *A* - ASTM D5766 open-hole tensile sample (geometry & boundary conditions)

B. *Mesh Description*

Three dimensional eight node brick continuum elements with reduced integration (C3D8R) were used. The model was partitioned at particular segments in order to apply boundary conditions, and apply refined mesh around the central hole. Figure 2 shows the used mesh with special focus on the hole region.

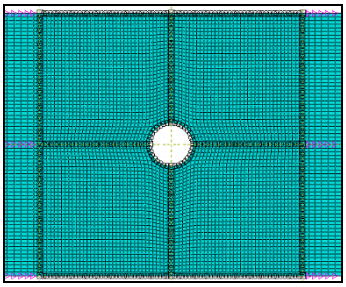

Figure 2: Open-hole model mesh

C. Material Modelling

Material properties (fibre & matrix), ply thickness, and ply orientation were defined using the "Create Composite Material" plugin available in ABAQUS/Standard V6.12. The Autodesk Composite Material Manager was utilized to define and optimize the composite properties based on the constituents' properties that were obtained from the literature. Table 1 presents the composite material properties, after optimization, based on E-Glass fibre and polyester resin properties that were obtained from [32] and [33], respectively. All samples were assumed to have a fibre volume fraction (V_F) of 50%; this was based on experimental trials and previously published data [34].

Table 1: Material properties

Elastic Properties	E_{11} (Pa)	E_{22} (Pa)	E_{33} (Pa)
	3.765E+10	9.233E+09	9.233E+09
	G_{12} (Pa)	G_{13} (Pa)	G_{23} (Pa)
	3.228E+09	3.228E+09	3.131E+09
	ν_{12}	ν_{13}	ν_{23}
	0.282	0.282	0.474
Failure Stresses	$^{+}\sigma_{11}$ (Pa)	$^{-}\sigma_{11}$ (Pa)	σ_{12} (Pa)
	1.075E+09	-7.250E+08	1.182E+08
	$^{+}\sigma_{22}$ (Pa)	$^{-}\sigma_{22}$ (Pa)	σ_{13} (Pa)
	5.752E+07	-2.825E+08	1.182E+08
	$^{-}\sigma_{33}$ (Pa)	σ_{33} (Pa)	σ_{23} (Pa)
	5.752E+07	-2.825E+08	9.417E+07

In order to model progressive failure of different composite constituents (fibre and matrix), the MCT – available in ASCA – was used. Stress-based failure criterion with instantaneous material property degradation was used, where post failure degradation (PFD) values are assigned to the constituent elastic matrix when failure occurs. In other words, the value of a PFD parameter represents the magnitude of the damaged elastic modulus as a fraction of the undamaged one. In the current work, the default ASCA PFD values were used, where the matrix post failure degradation (MPFD) and fibre post failure degradation (FPFD) parameters were 0.1 and 0.01, respectively. It is important to note that, the PFD values depend on the composite type (woven or unidirectional), fibre/matrix combination as well as loading conditions [35].

III. RESULTS AND DISCUSSION

In order to visualize different modes of failure, different state variables (SDVs), available in Abaqus/Standard, were requested. Only SDV1 is presented in the current paper. SDV1 is a real variable that represents the discrete damage state of a composite material, by assuming a finite number of discrete values between 1 and 3. A value of 1 means that there is no failure in the composite, a value of 2 means that there is matrix failure, and a value of 3 means that there is fibre failure.

A. Model Validation

The current ASTM D5766 open-hole model (Model *A*) has been validated for plain woven GFRP laminates, by comparing the predicted stress-strain curve to the experimental stress-curve of Shindo et al. [36], in a previous article by the current authors [37]. Since the current article deals with unidirectional GFRP laminates, whose mechanics are much simpler than woven laminates, such validation has been considered sufficient. In addition, the current results have been supported by basic stress analysis concepts as well as previously published data, as demonstrated below.

B. Global Failure Analysis

1. Load Carrying Capacity

Figure 3 presents the global load-displacement response of the different composite laminates. All four cases are shown; the open-hole and virgin models with both ply orientations ($[0/90]_{2S}$ and $[\pm45]_{2S}$). As can be seen, the load carrying capacity (maximum load: F_{max}) for the $[0/90]_{2S}$ laminates is much greater than the $[\pm45]_{2S}$ laminates. This applies to both open-hole and virgin samples, with different proportions, and could be simply explained in terms of local stress components (σ_{11}, σ_{22} and σ_{12}). Using the simple stress transformation matrix, given by Equation (1), local stress states could be found, where the $[0/90]_{2S}$ laminates are subjected to a uniaxial local tensile stress state: $\sigma_{11} = \sigma_X$, $\sigma_{22} = 0$ and $\sigma_{12} = 0$. On the other hand, the $[\pm45]_{2S}$ laminates are subjected to an equal biaxial local tensile and shear stress state: $\sigma_{11} = \sigma_{22} = \sigma_{12} = 0.5\ \sigma_X$.

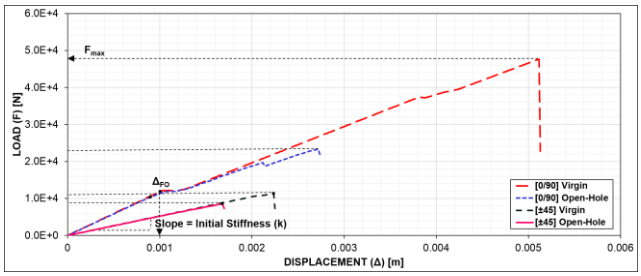

Figure 3: Load-displacement curves of open-hole & virgin models (Model *A* & Model *B*, respectively)

$$\begin{bmatrix}\sigma_{11}\\ \sigma_{22}\\ \sigma_{12}\end{bmatrix} = \begin{bmatrix}\cos\theta^2 & \sin\theta^2 & 2\cos\theta\sin\theta\\ \sin\theta^2 & \cos\theta^2 & -2\cos\theta\sin\theta\\ -\cos\theta\sin\theta & \cos\theta\sin\theta & \cos\theta^2-\sin\theta^2\end{bmatrix}\begin{bmatrix}\sigma_X\\ \sigma_Y\\ \sigma_{XY}\end{bmatrix} \quad (1)$$

Where θ is the angle between local (1-2) and global (X-Y) stress components, as shown in Figure 4.

Comparing the maximum local stress components of the $[0/90]_{2S}$ laminates to those of the $[\pm45]_{2S}$ laminates, for each of the different composite constituents (fibres and matrix); it

could be concluded that failure of the $[\pm45]_{2S}$ laminates would be matrix dominated while that of the $[0/90]_{2S}$ laminates would be fibre-dominated. This is basically because the matrix of the $[\pm45]_{2S}$ laminates is subjected to a shear stress that is equal to the tensile fibre stress components. On the other hand, the matrix of the $[0/90]_{2S}$ laminates is stress free. Since polymer matrices are much weaker than glass fibres, failure of the $[\pm45]_{2S}$ laminates would be matrix dominated and their load carrying capacity would be much lower than that of the $[0/90]_{2S}$ laminates.

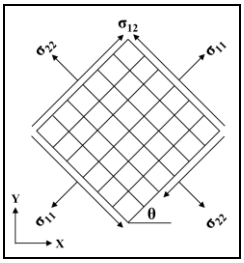

Figure 4: Local and global stress components (stress transformation)

In FRP composite laminates, stress concentration effects are function of ply orientation, stacking sequence as well as materials properties (matrix, fibres, and matrix-fibre interface) [38]. Figure 5 compares the load carrying capacity (F_{max}) of all cases, where the ratio between the virgin and open-hole samples for $[0/90]_{2S}$ and $[\pm45]_{2S}$ laminates is 2.0 and 1.3, respectively. Noting that the ratio between the load-carrying area of virgin to open-hole models is 1.2; therefore, the equivalent stress concentration factor (K_T) for $[0/90]_{2S}$ and $[\pm45]_{2S}$ laminates would be 1.7 and 1.1, respectively. In other words, the hole has insignificant stress concentration effects on the $[\pm45]_{2S}$ laminates, while it results in an increase of about 70% in the $[0/90]_{2S}$ laminates. The same trend was also shown in [39]. Again, the effect of fibre orientation on stress concentration could be explained in terms of the local stress state of each laminate.

Considering a metallic plate of an infinite width with a central hole of radius (a) under uniaxial tensile loading (σ), local stress distribution around the hole is given by Equation (2) [40]. Using Equation (2), the following local stresses – of interest – could be found; $\sigma_0 = -\sigma$, $\sigma_{90} = 3\sigma$, $\sigma_{45} = \sigma_{-45} = \sigma$. In case of equal biaxial loading and using the superposition principle, the overall local stresses would be $\sigma_0 = \sigma_{90} = 2\sigma$. Since the current $[0/90]_{2s}$ laminates are subjected to a uniaxial local stress state ($\sigma_{11} = \sigma$, $\sigma_{22} = \sigma_{12} = 0$), while the $[\pm45]_{2S}$ laminates are subjected to a biaxial stress state ($\sigma_{11} = \sigma_{22} = 0.5\ \sigma$ and $\sigma_{12} = 0.5\ \sigma$); therefore, only the $[0/90]_{2s}$ laminates would experience stress concentration effects. This agrees with the current results presented above.

$$\sigma_\theta = \frac{\sigma}{2}\left[1+\frac{a^2}{r^2} - \left(1+3\frac{a^4}{r^4}\right)\cos(2\theta)\right] \quad (2)$$

Where,
σ_θ is the stress at an angle (θ) from the loading (σ) direction
a is the radius of the circular hole
r is the radius of the point of interest from the center of the hole

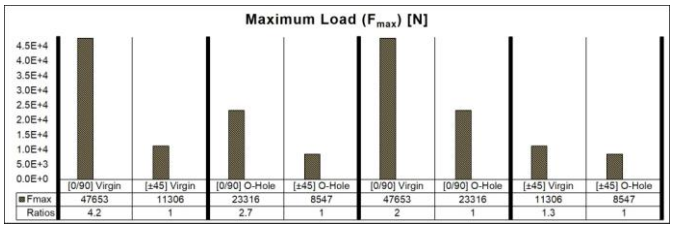

Figure 5: Load carrying capacity (F_{max}) of different cases

2. Initial Stiffness

Figure 6 compares the initial stiffness (slope of load-displacement curve) for different cases. The initial stiffness is defined as the stiffness of the sample before failure onset; i.e., before experiencing any failure features. It is important to note that, both the open-hole and virgin samples have almost the same initial stiffness. In other words, stress concentration effects do not have an impact on stiffness. This could be attributed to the fact that stress concentration effects are typically much localized, and do not extend to global stiffness.

Evaluating the effect of fibre orientation, the stiffness of the $[0/90]_{2S}$ laminates was found to be almost double that of the $[\pm45]_{2S}$ laminates. This applies to the open-hole as well as virgin samples. This could be explained in the same way as load carrying capacity and using the stress transformation matrix. Due to the different local stress state between $[0/90]_{2S}$ and $[\pm45]_{2S}$ laminates, and since glass fibres are much stiffer than polymer matrices; therefore, the $[0/90]_{2S}$ laminates would be stiffer than the $[\pm45]_{2S}$ laminates.

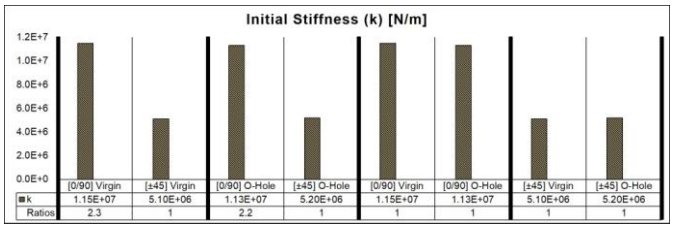

Figure 6: Initial stiffness of different cases

C. Progressive Failure Analysis

The current section focuses on analysing the progressive failure features of composite constituents, and how they explain the aforementioned global failure analysis results.

1. Cross Layers: $[0/90]_{2S}$ Laminates

Figure 7 demonstrates the progressive stiffness degradation experienced by the $[0/90]_{2s}$ laminates, before complete failure. Failure starts with matrix cracking at about 16% F_{max} (state 1), followed by fibre failure at about 62% F_{max} (state 2). Before any fibre failure took place (between state 1 and state 2), the overall sample stiffness experienced a drop of about 22%, which is attributed to progressive matrix cracking. Figure 8 shows different progressive failure features, starting with the first matrix failure (state 1) and ending by complete composite failure (state 5). As the load

increased, further stiffness degradation (about 19%) took place until fibre failure took place across the whole sample width (state 3), at about 80% F_{max}. Further increase in load (up to state 4: right before 100% F_{max}) did not result in any significant drop in sample stiffness. At full load (state 5), the composite laminate totally lost its load carrying capability, with severe damage and stiffness loss.

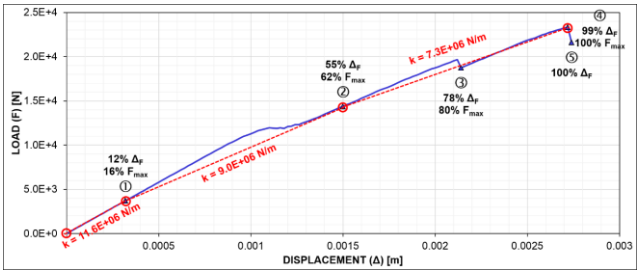

Figure 7: Progressive stiffness degradation of open-hole $[0/90]_{2s}$ laminates

Taking a closer look at different progressive failure features (Figure 8) shows that, initial matrix cracking (state 1) took place only in the 90° plies (plies with fibres normal to the load direction); these were plies 1, 3, 6 and 8. This is basically because the fibres of these plies are stress free (σ_{22}=0), as demonstrated earlier, which leaves the matrix to take the load. On the other hand, the fibres actually carry the load in the other plies (parallel to load direction: 0^o plies), where σ_{11}= σ. At state 2, the composite laminates experienced the first fibre failure that took place in the 0° plies. At state 3, there is a significant increase in the percentage of failed fibres in the 0° plies, which extends across almost the whole sample width. It is important to note that such localized fibre failure has not yet prevented the composite laminate from responding to increased displacement load. When the load reaches state 4, the structure reaches almost complete failure, with fibre failures across the whole width.

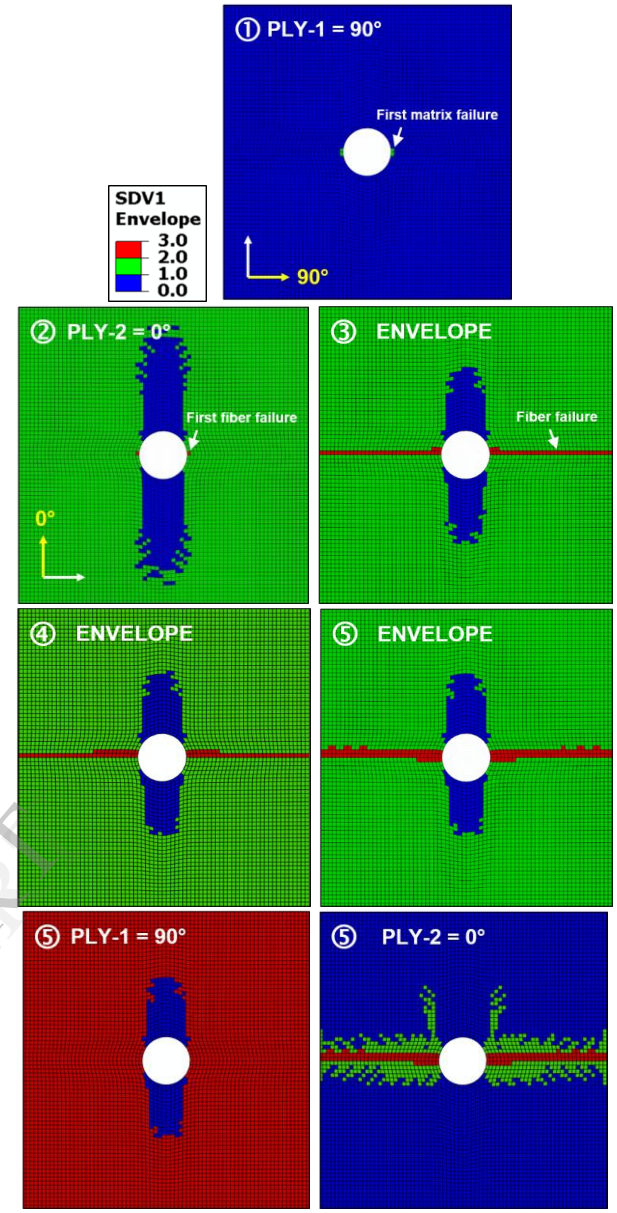

Figure 8: Progressive failure of open-hole $[0/90]_{2s}$ laminates – SDV1 shown

2. Angle Layers: $[\pm 45]_{2S}$ Laminates

Figure 9 presents the load-displacement response of the $[\pm 45]_{2s}$ laminates, with a close look at stiffness degradation. It is obvious that, the overall response seems to be linear with minimal stiffness degradation (about 6%) before complete failure. Stiffness degradation started with the first evidence of matrix cracking (state 1), at a load about 61% F_{max}. It is important to note that; only matrix cracking took place without any fibre failure, as shown in Figure 10. Also, matrix cracking took place along the fibres directions (45 degrees), which agrees with well-established failure features of FRP, where matrix cracking is typically guided by fibres.

The current results could be clearly explained in terms of the local stress state of the $[\pm 45]_{2s}$ laminates ($\sigma_{11} = \sigma_{22} = 0.5\ \sigma$ and $\sigma_{12} = 0.5\ \sigma$). Since both the fibres and matrix are subjected to the same stress level, and the matrix shear

strength is much lower than the tensile strength of fibres; matrix cracking would be definitely the dominant failure mechanism. This is clearly supported by the progressive failure features (matrix cracking) shown in Figure 10. Also, since the matrix contribution to the overall sample stiffness is minimal compared to fibres, and since matrix cracking was the only failure mechanism experienced; this explains the minimal and gradual drop in the overall sample stiffness, which is totally different from the $[0/90]_{2s}$ behaviour.

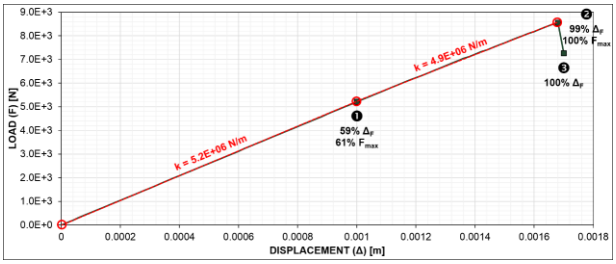

Figure 9: Progressive stiffness degradation of open-hole $[\pm45]_{2s}$ laminates

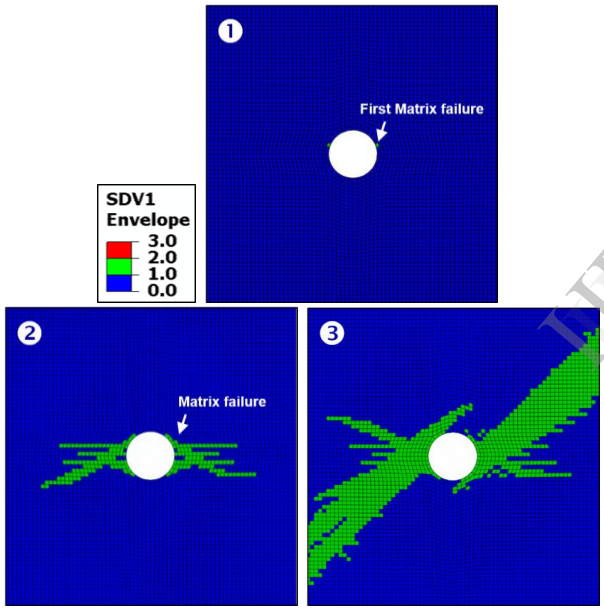

Figure 10: Progressive failure of open-hole $[\pm45]_{2s}$ laminates – SDV1 shown

IV. CONCLUSION

Based on the current results, the following conclusions were drawn.

- The current FE model, with the aid of MCT approach, has successfully modelled the stress concentration effects of a central hole on the mechanical behaviour of unidirectional GFRP laminates, with two ply orientations; $[0/90]_{2S}$ and $[\pm45]_{2S}$.
- The stress concentration effects in GFRP laminates highly depend on fibre orientation. This is because stress concentration effects depend mainly on local stress components rather than global ones. For the studied cases, for samples with hole-to-width ratio of 6:
  - The $[0/90]_{2S}$ laminates ($\sigma_{11} = \sigma$, $\sigma_{22} = \sigma_{12} = 0$) experienced an increase in local stresses by about 70%. In other words, a decrease in their load carrying capacity by about 70%.
  - On the other hand, the $[\pm45]_{2S}$ laminates ($\sigma_{11} = \sigma_{22} = 0.5\ \sigma$ and $\sigma_{12} = 0.5\ \sigma$) experienced no stress concentration effects.
- A central hole has an insignificant effect on the sample initial stiffness (before failure onset). This applies to both laminates: $[0/90]_{2S}$ and $[\pm45]_{2S}$, and is attributed to the localized effects of the hole, which do not extend to affects the sample's overall stiffness.
- When matrix cracking is the dominant failure mechanism, the FRP laminates experience gradual and minimal stiffness degradation before complete failure. On the other hand, when fibres failure occur significant stiffness degradation takes place before complete failure.
- The $[0/90]_{2S}$ laminates (both open-hole and virgin) have a much higher load carrying capacity and stiffness compared to the $[\pm45]_{2S}$ laminates. Again, this was explained in terms of local stress components.

ACKNOWLEDGMENT

The authors would like to thank the Ministry of Higher Education (MOHE) – Egypt for their financial support for performing the current research. Also, they would like to thank the Japan International Cooperation Agency (JICA) for their continuous support to the Egypt-Japan University of Science and Technology (E-JUST).

REFERENCES

[1] P. P. Camanho, P. Maimí, and C. G. Dávila, "Prediction of size effects in notched laminates using continuum damage mechanics," *Composites Science and Technology*, vol. 67, no. 13, pp. 2715–2727, Oct. 2007.

[2] M. J. Hinton and P. D. Soden, "Predicting failure in composite laminates: the background to the exercise," *Composites Science and Technology*, vol. 58, no. 7, pp. 1001–1010, Jul. 1998.

[3] M. J. Hinton and A. S. Kaddour, "The background to Part B of the Second World-Wide Failure Exercise: Evaluation of theories for predicting failure in polymer composite laminates under three-dimensional states of stress," *Journal of Composite Materials*, p. 0021998312473346, Jan. 2013.

[4] J. Echaabi, F. Trochu, and R. Gauvin, "Review of failure criteria of fibrous composite materials," *Polym Compos*, vol. 17, no. 6, pp. 786–798, Dec. 1996.

[5] M. Nasr, M. N. Abouelwafa, A. Gomaa, A. Hamdy, and E. Morsi, "A New Failure Criterion for Woven-Roving Fibrous Composites Subjected to Tension-Compression Local Plane Stresses With Different Stress Ratios," *J. Eng. Mater. Technol.*, vol. 127, no. 1, pp. 130–135, Feb. 2005.

[6] C. C. Chamis, "Polymer Composite Mechanics Review — 1965 to 2006," *Journal of Reinforced Plastics and Composites*, vol. 26, no. 10, pp. 987–1019, Jul. 2007.

[7] F.-K. Chang and K.-Y. Chang, "A Progressive Damage Model for Laminated Composites Containing Stress Concentrations," *Journal of Composite Materials*, vol. 21, no. 9, pp. 834–855, Sep. 1987.

[8] S. C. Tan, "A Progressive Failure Model for Composite Laminates Containing Openings," *Journal of Composite Materials*, vol. 25, no. 5, pp. 556–577, May 1991.

[9] S. C. Tan and J. Perez, "Progressive Failure of Laminated Composites with a Hole under Compressive Loading," *Journal of Reinforced Plastics and Composites*, vol. 12, no. 10, pp. 1043–1057, Oct. 1993.

[10] P. P. Camanho and F. L. Matthews, "A Progressive Damage Model for Mechanically Fastened Joints in Composite Laminates," *Journal of Composite Materials*, vol. 33, no. 24, pp. 2248–2280, Dec. 1999.

[11] M. M. Shokrieh and L. B. Lessard, "Progressive Fatigue Damage Modelling of Composite Materials, Part I: Modelling," *Journal of Composite Materials*, vol. 34, no. 13, pp. 1056–1080, Jul. 2000.
[12] M. M. Shokrieh and L. B. Lessard, "Progressive Fatigue Damage Modelling of Composite Materials, Part II: Material Characterization and Model Verification," *Journal of Composite Materials*, vol. 34, no. 13, pp. 1081–1116, Jul. 2000.
[13] K. I. Tserpes, G. Labeas, P. Papanikos, and T. Kermanidis, "Strength prediction of bolted joints in graphite/epoxy composite laminates," *Composites Part B: Engineering*, vol. 33, no. 7, pp. 521–529, Oct. 2002.
[14] I. Lapczyk and J. A. Hurtado, "Progressive damage modelling in fibre-reinforced materials," *Composites Part A: Applied Science and Manufacturing*, vol. 38, no. 11, pp. 2333–2341, Nov. 2007.
[15] G. Belingardi, E. G. Koricho, and A. T. Beyene, "Characterization and damage analysis of notched cross-ply and angle-ply fabric GFRP composite material," *Composite Structures*, vol. 102, pp. 237–249, Aug. 2013.
[16] S. Yashiro, K. Murai, T. Okabe, and N. Takeda, "Numerical study for identifying damage in open-hole composites with embedded FBG sensors and its application to experiment results," *Advanced Composite Materials*, vol. 16, no. 2, pp. 115–134, 2007.
[17] H. Suemasu, H. Takahashi, and T. Ishikawa, "On failure mechanisms of composite laminates with an open hole subjected to compressive load," *Composites Science and Technology*, vol. 66, no. 5, pp. 634–641, May 2006.
[18] H. Suemasu, Y. Naito, K. Gozu, and Y. Aoki, "Damage initiation and growth in composite laminates during open hole compression tests," *Advanced Composite Materials*, vol. 21, no. 3, pp. 209–220, 2012.
[19] G. Sadeghi, H. Hosseini-Toudeshky, and B. Mohammadi, "An investigation of matrix cracking damage evolution in composite laminates – Development of an advanced numerical tool," *Composite Structures*, vol. 108, pp. 937–950, Feb. 2014.
[20] R. M. O'Higgins, M. A. McCarthy, and C. T. McCarthy, "Comparison of open hole tension characteristics of high strength glass and carbon fibre-reinforced composite materials," *Composites Science and Technology*, vol. 68, no. 13, pp. 2770–2778, Oct. 2008.
[21] Eugene Dan-Jumbo, Russell Keller, Wen S. Chan, Selvaraj S., "STRENGTH OF COMPOSITE LAMINATE WITH MULTIPLE HOLES," in *ICCM-17 Edinburgh*, Edinburgh, UK, 2009.
[22] F.-K. Chang and K.-Y. Chang, "A Progressive Damage Model for Laminated Composites Containing Stress Concentrations," *Journal of Composite Materials*, vol. 21, no. 9, pp. 834–855, Sep. 1987.
[23] S. R. Hallett and M. R. Wisnom, "Experimental Investigation of Progressive Damage and the Effect of Layup in Notched Tensile Tests," *Journal of Composite Materials*, vol. 40, no. 2, pp. 119–141, Jan. 2006.
[24] B. M. Zhang and L. Zhao, "Progressive Damage and Failure Modelling in Fibre-Reinforced Laminated Composites Containing a Hole," *International Journal of Damage Mechanics*, p. 1056789511423951, Oct. 2011.
[25] F. Yang and C. L. Chow, "Progressive Damage of Unidirectional Graphite/Epoxy Composites Containing a Circular Hole," *Journal of Composite Materials*, vol. 32, no. 6, pp. 504–525, Mar. 1998.
[26] "Lighter, stronger, more efficient design. Get better answers with HELIUS:MCTTM." [Online]. Available: http://www.firehole.com/documents/mct_flyer.pdf.
[27] R. Hill, "Elastic properties of reinforced solids: Some theoretical principles," *Journal of the Mechanics and Physics of Solids*, vol. 11, no. 5, pp. 357–372, Sep. 1963.
[28] Jeffry S. Welsh, J. Steve Mayes, and Adam C. Biskner, "Experimental and numerical failure predictions of biaxially-loaded quasi-isotropic carbon composites," presented at the 16th International Conference on Composite Materials.
[29] J. Andrew, C. Hansen, Steven Mayes, "Multicontinuum Failure Analysis of Composite Structural Laminates," *Mechanics of Composite Materials and Structures*, vol. 8, no. 4, pp. 249–262, 2001.
[30] J. S. Mayes and A. C. Hansen, "A comparison of multicontinuum theory based failure simulation with experimental results," *Composites Science and Technology*, vol. 64, no. 3–4, pp. 517–527, Mar. 2004.
[31] "Intelligent Discrete Softening Method (IDS Method)" [Online]. Available: http://www.firehole.com/products/mct/isdm.aspx.
[32] "S-2 Glass Fibre", Owens-Corning Fibreglass Corporation, Pub. No. 15-PL-16154, (March 1990).
[33] "1992 Materials Selector," Materials Engineering, p. 181, (December 1991).
[34] Clarke, J. L. (Ed.). (2003). Structural design of polymer composites: Eurocomp design code and background document. CRC Press.
[35] "Helius:MCT 3.0 Tech Brief." [Online]. Available: http://www.deskeng.com/pics/pdfs/HeliusMCT3TechBrief.pdf.
[36] Y. Shindo, S. Watanabe, T. Takeda, F. Narita, T. Matsuda, and S. Yamaki, "Numerical and experimental evaluation of cryogenic tensile strength of woven fabric-reinforced glass/epoxy composites using open hole specimens," *Journal of Mechanics of Materials and Structures*, vol. 6, no. 1–4, pp. 545–556, Jun. 2011.
[37] A. Abdalla, A. Abdelmoneim & M. Nasr, "Modelling the Effects of Fibre Orientation on the Mechanical Behaviour of Plain Woven GFRP Open-hole Laminates under Tensile Loading", *Composites Part B: Engineering* – under review.
[38] E. Armanios and J. Reeder, American Society for Composites / American Society for Testing And Materials Committee D30: Nineteenth Technical Conference. DEStech Publications, Inc, 2004.
[39] W. Young and R. Budynas, *Roark's Formulas for Stress and Strain*, 7 edition. New York: McGraw-Hill Professional, 2001.
[40] J. R. Davis, *Tensile Testing*. ASM International, 2004.